

Metal–organic coordination architectures of bis(*N*-imidazolyl) pyridazine: Syntheses, structures, emission and photocatalytic properties

Duo-Zhi Wang ^{a,b,*}, Jin-Ping Li ^b, Jian-Zhong Fan ^b, Dian-Zeng Jia ^a

^a Key Laboratory of Material and Technology for Clean Energy, Ministry of Education, Institute of Applied Chemistry, Xinjiang University, Urumqi, 830046 Xinjiang, PR China

^b College of Chemistry and Chemical Engineering, Xinjiang University, Urumqi 830046, PR China



ARTICLE INFO

Article history:

Received 25 January 2016

Accepted 12 March 2016

Available online 22 March 2016

Keywords:

Bis(*N*-imidazolyl) pyridazine

Complex

Crystal structure

Emission properties

Photocatalytic

ABSTRACT

In efforts to explore the effects of metal ions, counter anions on the structures and properties of metal–organic complexes, seven new complexes $[\text{ZnL}(\text{OH})_2]$ (**1**), $\{\text{[ZnL(AcO)}_2](\text{CH}_3\text{CH}_2\text{OH})\}_{\infty}$ (**2**), $\{\text{[ZnL(H}_2\text{O)}_4](\text{SO}_4)\}_{\infty}$ (**3**), $[\text{CdL}_4(\text{OH})_2]$ (**4**), $\{\text{[CdL(AcO)}_2](\text{CH}_3\text{CH}_2\text{OH})\}_{\infty}$ (**5**), $\{\text{[CdL(H}_2\text{O)}_4](\text{SiF}_6)\}_{\infty}$ (**6**) and $\{\text{[Cu}_2\text{L}_2(\text{SO}_4)_2(\text{H}_2\text{O})_2](\text{H}_2\text{O})\}_{\infty}$ (**7**) [**L** = 3,6-bis(*N*-imidazolyl) pyridazine] were synthesized and structurally characterized by elemental analyses, IR spectroscopy and single-crystal X-ray diffraction. Complexes **1** and **4** have similar mononuclear structures. Complexes **2**, **3** and **6** have 1-D chain structures, while **5** reveals 2-D neutral infinite sheet structure. One 1-D chain and one 2-D sheet form complicated structure of complex **7**. The ligands **L** adopt didentate bridging mode to coordinate to the metal ions in complexes **2**, **3**, and **5–7**. Obviously, the structural differences among them are attributable to the differences of metal ions, counter anions and coordination modes of ligand. The fluorescent property of complexes **1–6** have been investigated and discussed. In addition, complexes **1–5** exhibit photocatalytic activity and selectivity for dye degradation under UV light.

© 2016 Elsevier Ltd. All rights reserved.

1. Introduction

Metal–organic frameworks (MOFs) are currently of great interest [1], not only for their intriguing topological variety and the convenient synthesis from organic ligands and metal ions through a modular approach [2], but also they were widely regarded as promising materials for many applications [3], such as catalysis, separation, gas storage, sensing, magnetism, drug delivery, ionic/molecular recognition and ion exchange [4,5]. However, the final structure of metal–organic frameworks (MOFs) can be influenced by multiple factors such as the coordination geometry of metal center, the nature of the ligand, counter anions, the ratio of ligand to metal ion, temperature, solvent system, pH value and so on [6,7]. Among the various factors, the selection of organic ligands is a very important consideration [8]. The configuration, flexibility and coordination mode of organic ligands have been identified to be the most critical factors to the fine-tuning of molecular skeletons [9]. Up to now, a great number of inorganic–organic hybrid coordination polymers have been

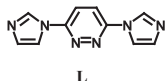
reported based on the ligands containing N donors such as pyridine [10], imidazole [11], tetrazole [12] and triazole [13] etc. Previously, we reported a series of N-containing heterocyclic ligands and complexes [14,15], some of which can emit blue luminescence.

Imidazole and its derivatives are potential multi-topic ligands in constructing coordination complexes [16]. A large number of oligonuclear and polynuclear metal coordination compounds with imidazole derivatives with luminescent properties and novel topologies have been reported [17,18]. The ligands of benzene ring substituted by imidazole or benzimidazole can adopt different conformations when forming metal complexes according to the different geometric requirements of metal centers [19,20]. Many complexes with these ligands show unique structures, such as 3-D frameworks, 2-D networks, 1-D chains, 0-D clusters and exhibit interesting properties. But, the research on the rigid ligands composed by pyridazine ring directly bridging imidazole groups was less reported.

In this work, we carried out research on the coordination chemistry of pyridazine containing ligand, we designed and synthesized ligand 3,6-bis(*N*-imidazolyl) pyridazine (**L**) (Chart 1) and successfully prepared two mononuclear complexes namely, $[\text{ZnL}(\text{OH})_2]$ (**1**) and $[\text{CdL}_4(\text{OH})_2]$ (**4**), five novel coordination polymers, namely,

* Corresponding author at: College of Chemistry and Chemical Engineering, Xinjiang University, Urumqi, 830046, PR China.

E-mail address: wangdz@xju.edu.cn (D.-Z. Wang).

**Chart 1.** The structure of ligand **L**.

$\{[\text{ZnL}(\text{AcO})_2](\text{CH}_3\text{CH}_2\text{OH})\}_{\infty}$ (**2**), $\{[\text{ZnL}(\text{H}_2\text{O})_4](\text{SO}_4)\}_{\infty}$ (**3**), $\{[\text{CdL}(\text{AcO})_2](\text{CH}_3\text{CH}_2\text{OH})\}_{\infty}$ (**5**), $\{[\text{CdL}(\text{H}_2\text{O})_4](\text{SiF}_6)\}_{\infty}$ (**6**) and $\{[\text{Cu}_2\text{L}_2(\text{SO}_4)_2(\text{H}_2\text{O})_2](\text{H}_2\text{O})\}_{\infty}$ (**7**). Interestingly, these compounds exhibit various network architectures with a wide range from 0D to 2D networks. The metal ions and the counter anions play important roles in the construction of the final structures and their effects will be discussed in detail. Furthermore, the luminescent property and photocatalytic activity of the complexes **1–6** have been investigated and discussed, and complexes **1–5** exhibit photocatalytic activity and selectivity for dye degradation under UV light.

2. Experimental

2.1. Materials and general methods

All the other reagents used for the syntheses were commercially available and employed without further purification. IR spectra were measured on a Brucker Equinox 55 FT-IR spectrometer with KBr Pellets in the range of 4000–400 cm⁻¹. Elemental analyses of C, H and N were performed on a Thermo Flash EA 1112-NCHS-O analyzer. ¹H NMR data were collected using an INOVA-400 NMR spectrometer. Chemical shifts are reported in δ relative to TMS. The fluorescence behavior of ligand and their complexes were studied using a Hitachi F-4500 Fluorescence Spectrophotometer with a Xe arc lamp as the light source and bandwidths of 2.5 nm at room temperature. UV-Vis absorption spectra were obtained using a Hitachi UV-3010 UV-Vis spectrophotometer. The X-ray powder diffraction (XRPD) was recorded on a Rigaku D/Max-2500 diffractometer at 40 kV, 100 mA for a Cu-target tube and a graphite monochromator.

2.2. Preparation of ligand **L**

Imidazole (3.4 g, 49.9 mmol), sodium (1.2 g, 52.2 mmol) and 80 mL THF was added to a 250 mL three-necked flask. The solution was heated to reflux for 40 min. A solution of 3,6-dichloropyridazine (3.7 g, 24.8 mmol) in THF (10 mL) was added to the mixture within 40 min. The mixture was refluxed for 4 h under N₂. The reaction mixture was poured into ice water mixture after cooled to room temperature. The earthy yellow solid of **L** was obtained after filtering. Pure ligand **L** was obtained by recrystallization from ethanol as white crystals. Yield 80%. m.p. 281–282 °C. ¹H NMR (DMSO-*d*₆): δ: 8.69 (s, 2H, imidazole-2), 8.48 (s, 2H, pyridazine), 8.11 (d, 2H, *J* = 2.4 Hz, imidazole-5), 7.23 (d, 2H, *J* = 2.4 Hz, imidazole-4); Anal. Calc. for C₁₀H₈N₆: C, 56.60; H, 3.80; N, 39.60. Found: C, 56.75; H, 3.75; N, 39.54%. IR (cm⁻¹, KBr pellets): 3176w, 3145m, 3109m, 3047m, 3018m, 2946m, 2782w, 2621w, 2526w, 2408w, 2214w, 1991w, 1903w, 1795w, 1727w, 1692w, 1645w, 1577s, 1519s, 1490s, 1459s, 1371s, 1321s, 1277s, 1237s, 1163m, 1106m, 1059m, 1031s, 962m, 903m, 861s, 823s, 766s, 749s, 645s, 613m, 507w, 487m, 421m.

2.3. Syntheses of complexes **1–7**

2.3.1. $[\text{ZnL}_4(\text{OH})_2]$ (**1**)

A mixture of Zn(NO₃)₂·6H₂O (89 mg, 0.3 mmol) and **L** (63 mg, 0.3 mmol) and 5 mL water, which was placed in a Teflon-lined stainless steel vessel (25 mL) was heated to 140 °C for 3 days, then cooled to room temperature at a rate of 10 °C h⁻¹. Complex **1** was

obtained after filtering, washed with distilled water and dried in air to produce the colorless crystals (ca. 30% yield based on **L**). Anal. Calc. for C₄₀H₃₄N₂₄O₂Zn: C, 50.66; H, 3.61N, 35.45. Found: C, 50.48; H, 3.52; N, 35.65%. IR (cm⁻¹, KBr pellets): 3394m, 3115m, 2526w, 2416w, 2211w, 2081w, 1911w, 1871w, 1806w, 1522s, 1481s, 1318s, 1241s, 1148m, 1099m, 1064m, 1032m, 967m, 931m, 916m, 838m, 735m, 651m, 614m, 490m, 418m.

2.3.2. $[\text{ZnL}(\text{AcO})_2](\text{CH}_3\text{CH}_2\text{OH})\}_{\infty}$ (**2**)

A mixture of Zn(OAc)₂·2H₂O (7 mg, 0.03 mmol) and **L** (7 mg, 0.03 mmol) was dissolved in 15 mL ethanol and filtrated. The colorless block crystals were formed after several days with the evaporation of the filtrate. The crystalline product was obtained after filtering and washed with methanol (ca. 40% yield based on **L**). Anal. Calc. for C₁₆H₂₀N₆O₅Zn: C, 43.50; H, 4.56; N, 19.02. Found: C, 43.60; H, 4.42; N, 19.21%. IR (cm⁻¹, KBr pellets): 3267m, 3165m, 3115m, 3061m, 3027m, 2975m, 2930m, 2890m, 2841m, 2649w, 2544w, 2419w, 2340w, 2301w, 2248w, 2001w, 1918w, 1621s, 1589s, 1538m, 1488m, 1454s, 1379s, 1328s, 1308m, 1265m, 1245m, 1168m, 1150m, 1122m, 1096m, 1049m, 1018m, 966m, 941m, 926m, 887m, 850m, 758m, 720m, 674m, 647m, 619m, 494m, 433m.

2.3.3. $\{[\text{ZnL}(\text{H}_2\text{O})_4](\text{SO}_4)\}_{\infty}$ (**3**)

A mixture of ZnSO₄·7H₂O (7 mg, 0.02 mmol) and **L** (7 mg, 0.03 mmol) was dissolved in 15 mL solvent (H₂O: methanol = 2:1) and refluxed for 3 h. The colorless block crystals were formed after several days with the evaporation of the filtrate. The crystalline product was obtained after filtering and washed with distilled water (ca. 40% yield based on **L**). Anal. Calc. for C₁₀H₁₆N₆O₈Zn: C, 29.03; H, 3.89; N, 20.31. Found: C, 29.65; H, 3.58; N, 18.76%. IR (cm⁻¹, KBr pellets): 3175m, 3128m, 2356w, 2026w, 1923w, 1806w, 1646m, 1581m, 1493s, 1453s, 1303s, 1255m, 1069s, 967m, 929m, 834m, 760m, 645m, 616s, 532m, 494m, 444m.

2.3.4. $[\text{CdL}_4(\text{OH})_2]$ (**4**)

The colorless crystals of **4** suitable for X-ray analysis were obtained by the similar method described for **1**, except for using Cd(NO₃)₂·4H₂O instead of Zn(NO₃)₂·6H₂O. (ca. 35% yield based on **L**). Anal. Calc. for C₄₀H₃₄N₂₄O₂Cd: C, 48.27; H, 3.44; N, 33.78. Found: C, 48.70; H, 3.35; N, 33.65%. IR (cm⁻¹, KBr pellets): 3419m, 3182m, 3133m, 3109m, 3062m, 2524w, 2397w, 2211w, 2081w, 1996w, 1910w, 1805w, 1521m, 1483s, 1455m, 1306m, 1239m, 1157w, 1100m, 1061m, 1032m, 967m, 926m, 827m, 752m, 646m, 617m, 490m, 421m.

2.3.5. $[\text{CdL}(\text{AcO})_2](\text{CH}_3\text{CH}_2\text{OH})\}_{\infty}$ (**5**)

Complex **5** was synthesized similarly as **2** by using Cd(OAc)₂·2H₂O instead of Zn(OAc)₂·2H₂O. (ca. 40% yield based on **L**). Anal. Calc. for C₁₆H₂₀N₆O₅Cd: C, 39.32; H, 4.12; N, 17.19. Found: C, 39.67; H, 4.98; N, 17.33%. IR (cm⁻¹, KBr pellets): 3242m, 3183m, 3148m, 3129m, 3059m, 2975m, 2889m, 2840m, 2623w, 2486w, 2419w, 2321w, 1998w, 1918w, 1760w, 1683m, 1563s, 1535s, 1484s, 1455s, 1404s, 1311s, 1262m, 1166m, 1146m, 1118m, 1058s, 1034s, 967m, 931m, 883m, 843m, 760m, 744m, 674m, 648m, 618m, 495m, 428m.

2.3.6. $[\text{CdL}(\text{H}_2\text{O})_4](\text{SiF}_6)$ (**6**)

A mixture of CdSiF₆·6H₂O (7 mg, 0.02 mmol) and **L** (7 mg, 0.03 mmol) was dissolved in 15 mL solvent (H₂O: methanol = 1:1). The solution was refluxed for 3 h and allowed to evaporate for seven days and finally suitable colorless block crystals were formed. The crystalline product was obtained after filtering and washed with distilled water (ca. 45% yield based on **L**). Anal. Calc. for C₁₀H₁₆N₆O₄F₆SiCd: C, 22.29; H, 2.99; N, 15.60. Found: C,

22.60; H, 2.82; N, 15.48%. IR (cm^{-1} , KBr pellets): 3444m, 3167m, 3143m, 3090m, 2916w, 2879w, 2811w, 2775w, 2676w, 2630w, 2578w, 2535w, 2410w, 2341w, 2260w, 2225w, 2084w, 2029w, 1959w, 1910w, 1808w, 1641m, 1581m, 1499s, 1460s, 1364m, 1304s, 1264m, 1169m, 1130m, 1109m, 1065m, 1042m, 972m, 930m, 846m, 772m, 716m, 639m, 616m, 470m.

2.3.7. $\{\text{Cu}_2\text{L}_2(\text{SO}_4)_2(\text{H}_2\text{O})_2\}(\text{H}_2\text{O})\}_{\infty}$ (7)

The blue block crystals of **5** were obtained by the similar method described for **1** except for using $\text{CuSO}_4 \cdot 5\text{H}_2\text{O}$ instead of $\text{Zn}(\text{NO}_3)_2 \cdot 6\text{H}_2\text{O}$. (ca. 36% yield based on **L**). *Anal.* Calc. for $\text{C}_{20}\text{H}_{22}\text{N}_{12}\text{O}_{11}\text{S}_2\text{Cu}_2$: C, 30.11; H, 2.78; N, 21.07. Found: C, 30.35; H, 2.66; N, 21.18%. IR (cm^{-1} , KBr pellets): 3396m, 3137m, 2952m, 2923s, 2855m, 1957w, 1739w, 1651w, 1581m, 1549m, 1499m, 1460s, 1379m, 1328m, 1311m, 1268m, 1245m, 1195s, 1117s, 1056m, 1032m, 966m, 930m, 840m, 794m, 739m, 642m, 614s, 592m, 502m, 427m.

2.4. X-ray crystallography

Single-crystal X-ray diffraction measurements for complexes **1–7** were carried out on a Bruker APEX2 SMART CCD diffractometer equipped with a graphite crystal monochromator situated in the incident beam for data collection at 293(2) K. The determinations of unit cell parameters and data collections were performed with MoK α radiation ($\lambda = 0.71073 \text{ \AA}$) and unit cell dimensions were obtained with least-squares refinements. The program SAINT [21]

was used for integration of the diffraction profiles. All the structures were solved by direct methods using the SHELXS program of the SHELXTL package and refined by full-matrix least-squares methods with SHELXL [22]. Semi-empirical absorption corrections were carried out using SADABS program [23]. Metal atoms in the complexes were located from the *E*-maps and other non-hydrogen atoms were located in successive difference Fourier syntheses and refined with anisotropic thermal parameters on F^2 . The hydrogen atoms of the ligand were generated geometrically; and the hydrogen atoms of the water molecules were located from difference maps and refined with isotropic temperature factors. Crystal data and structure refinement parameters details for complexes **1–7** are given in Table 1.

3. Results and discussion

3.1. Syntheses and general characterizations

L was prepared in higher yield as white crystalline solid by the reaction of imidazole with 3,6-dichloropyridazine. The structure of **L** was determined by ^1H NMR, IR, elemental analysis. Complexes **1**, **4** and **7** were synthesized by the hydrothermal method at 140 °C without adding any base for adjusting the pH value. Complexes **3** and **6** were obtained in mixed solvent by refluxing, cooling and filtrating. Complexes **2** and **5** were obtained in organic solvent at room temperature.

Table 1
Crystal data and structure refinement summary for complexes **1–7**.

	1	2	3	4
Formula	$\text{C}_{40}\text{H}_{34}\text{ZnN}_{24}\text{O}_2$	$\text{C}_{16}\text{H}_{20}\text{ZnN}_6\text{O}_5$	$\text{C}_{10}\text{H}_{16}\text{N}_6\text{O}_8\text{S}\text{Zn}$	$\text{C}_{40}\text{H}_{34}\text{CdN}_{24}\text{O}_2$
Formular wt	948.27	441.75	445.72	995.33
Crystal system	orthorhombic	orthorhombic	monoclinic	tetragonal
Space group	<i>Aba</i> 2	<i>Pbca</i>	<i>P2(1)/n</i>	<i>I4(1)/acd</i>
<i>T</i> (K)	293(2)	296(2)	123(2)	293(2)
<i>a</i> (Å)	13.8229(3)	13.9535(4)	9.168(3)	14.0803(4)
<i>b</i> (Å)	13.8298(3)	10.5734(3)	9.161(3)	14.0803(4)
<i>c</i> (Å)	27.6093(6)	25.3448(8)	18.786(7)	55.315(2)
α (°)	90	90	90	90
β (°)	90	90	103.891(5)	90
γ (°)	90	90	90	90
<i>V</i> (Å ³)	5278.0(2)	3739.27(19)	1531.7(10)	10966.5(6)
<i>Z</i>	4	8	4	8
<i>D</i> (g cm ⁻³)	1.191	1.569	1.933	1.208
μ (mm ⁻¹)	0.521	1.356	1.801	0.452
<i>F</i> (000)	1944	1824	912	4064
Measured reflns	22992	22934	10860	21797
Obsd reflns	5615	3361	2949	3106
<i>R</i> ^a / <i>wR</i> ^b	0.0523/0.1925	0.0312/0.0833	0.0662/0.2385	0.0661/0.1870
	5	6	7	
Formula	$\text{C}_{16}\text{H}_{20}\text{CdN}_6\text{O}_5$	$\text{C}_{10}\text{H}_{16}\text{CdF}_6\text{N}_6\text{O}_4\text{Si}$	$\text{C}_{20}\text{H}_{22}\text{Cu}_2\text{N}_{12}\text{O}_{11}\text{S}_2$	
Formular wt	488.78	538.79	797.74	
Crystal system	orthorhombic	monoclinic	monoclinic	
Space group	<i>Pbca</i>	<i>P21/c</i>	<i>P21/c</i>	
<i>T</i> (K)	293(2)	293(2)	293(2)	
<i>a</i> (Å)	13.061(3)	8.6093(3)	12.352(7)	
<i>b</i> (Å)	10.383(2)	10.1421(3)	28.877(17)	
<i>c</i> (Å)	27.103(5)	20.9653(6)	7.727(4)	
α (°)	90	90	90	
β (°)	90	109.943	101.214(12)	
γ (°)	90	90	90	
<i>V</i> (Å ³)	3675.4(13)	1720.84(9)	2704(3)	
<i>Z</i>	8	4	4	
<i>D</i> (g cm ⁻³)	1.767	2.080	1.960	
μ (mm ⁻¹)	1.231	1.435	1.814	
<i>F</i> (000)	1968	1064	1616	
Measured reflns	32315	10935	16200	
Obsd reflns	4209	3139	4764	
<i>R</i> ^a / <i>wR</i> ^b	0.0214/0.0733	0.0264/0.0632	0.0371/0.0921	

^a $R = \sum(|F_{0l}| - |F_{cl}|)/\sum|F_{0l}|$.

^b $wR = [\sum w(|F_{0l}|^2 - |F_{cl}|^2)^2 / \sum w(F_{0l}^2)]^{1/2}$.

The infrared spectra of **1–7** exhibit characteristic absorptions for corresponding ligand with a slight shift due to coordination. The absorption bands at about 1069 cm^{-1} and 616 cm^{-1} indicate the existence of the free SO_4^{2-} anions in **3**. The characteristic bands of the coordinating SO_4^{2-} anions in **7** appear at 1117 cm^{-1} , 1056 cm^{-1} , 642 cm^{-1} , 614 cm^{-1} and 592 cm^{-1} , the reason is coordination interaction lead to symmetry decreases, the IR bands increase. Ligand **L** and complexes **1–7** all exhibited absorptions corresponding to the framework vibrations of aromatic rings at about $1450\text{--}1600\text{ cm}^{-1}$.

3.2. Crystal structures

3.2.1. $[\text{ZnL}_4(\text{OH})_2]$ (**1**) and $[\text{CdL}_4(\text{OH})_2]$ (**4**)

Structural analyses reveal that complexes **1** and **4** have similar OD structures. The coordination environment of Zn^{II} ion in **1** is also the same as that of Cd^{II} ion in **4**. Compounds **1** and **4** have the general formula of $\text{ML}_4(\text{OH})_2$ [$\text{M} = \text{Zn}$ (**1**), $\text{M} = \text{Cd}$ (**4**)]. Complex **1** crystallizes in orthorhombic space group $\text{Aba}2$, while complex **4** crystallizes in the tetragonal space group $I4(1)/acd$. Therefore, we just describe structure of complex **1**.

Crystallographic data and experimental details for structural analyses were summarized in Table 1, the selected bond distances and angles were listed in Table 1 of Supplementary 1. The X-ray diffraction analysis shows that **1** has a mononuclear structure (see Fig. 1). The Zn^{II} center is linked to four distinct imidazole N donors of four **L** ligands in the equatorial plane and two O atoms from two OH^- anions [$\text{Zn}(1)-\text{O}(1) = 2.121(3)\text{ \AA}$] at the axial positions to complete its distorted octahedron coordination geometry.

with the coordination angles varying from $86.63(16)^\circ$ to $179.4(3)^\circ$ (Fig. 1 and Supplementary 1). The $\text{Zn}(1)-\text{N}(2)$ and $\text{Zn}(1)-\text{N}(7)$ bond distances are $2.140(4)$ and $2.144(5)\text{ \AA}$, respectively, which are in the normal range. All the **L** ligands adopt monodentate coordination mode, and all the atoms of each ligand **L** are almost in the same plane.

3.2.2. $\{[\text{ZnL}(\text{AcO})_2](\text{CH}_3\text{CH}_2\text{OH})\}_\infty$ (**2**)

Complex **2** crystallizes in the orthorhombic space group $Pbca$ and the selected bond distances and angles were listed in Table 1 of Supplementary 1. The X-ray diffraction analysis shows that **2** has an infinite 1-D chain structure and all the Zn^{II} centers and **L** in **2** are equivalent (see Fig. 2), the asymmetric unit consists of one Zn^{II} center, one ligand **L**, two $\text{CH}_3\text{COO}^{2-}$ anions and one free $\text{CH}_3\text{CH}_2\text{OH}$ molecule. Different from complex **1**, the $\text{CH}_3\text{COO}^{2-}$ anions in **2** not only taken part in coordination, but also acted as counter anions for charge balance, the Zn^{II} ion is fourcoordinated to two O atoms of two distinct acetate anions [$\text{Zn}(1)-\text{O}(2) = 1.9739(19)\text{ \AA}$, $\text{Zn}(1)-\text{O}(4) = 1.980(2)\text{ \AA}$] and two N donors from two distinct **L** ligands [$\text{Zn}-\text{N}$ lengths are $2.018(2)$ and $2.029(2)\text{ \AA}$, respectively] to form a distorted tetrahedral geometry. The angles of $\text{N}(1)-\text{Zn}(1)-\text{N}(6)$ and $\text{O}(2)-\text{Zn}(1)-\text{O}(4)$ are $114.93(9)^\circ$ and $101.87(9)^\circ$, respectively, while $\text{N}-\text{Zn}-\text{O}$ angles are rang of from $95.15(8)^\circ$ to $125.77(9)^\circ$. Besides, the ligands adopted bidentate bridging modes coordinated to two Zn^{II} centers and extend to a 1-D chain. The neighboring non-bonding $\text{Zn}\cdots\text{Zn}$ distance connected by **L** is 13.288 \AA . All the atoms are almost in the same plane in each **L**, and the mean deviations from the planes of **L** are ca. 0.0554 \AA .

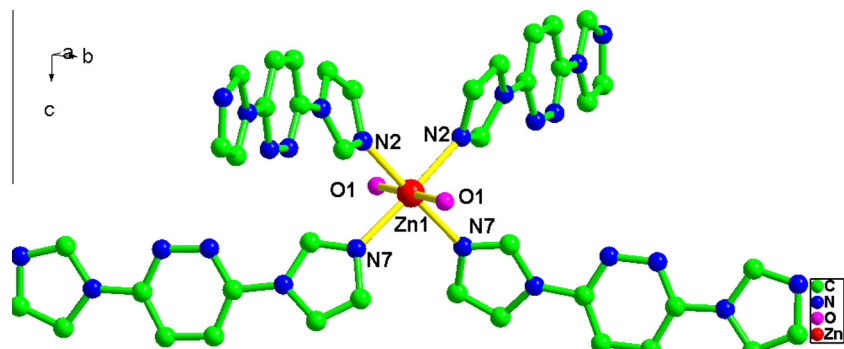


Fig. 1. View of the coordination environment of Zn^{II} ion in **1** (H atoms omitted for clarity).

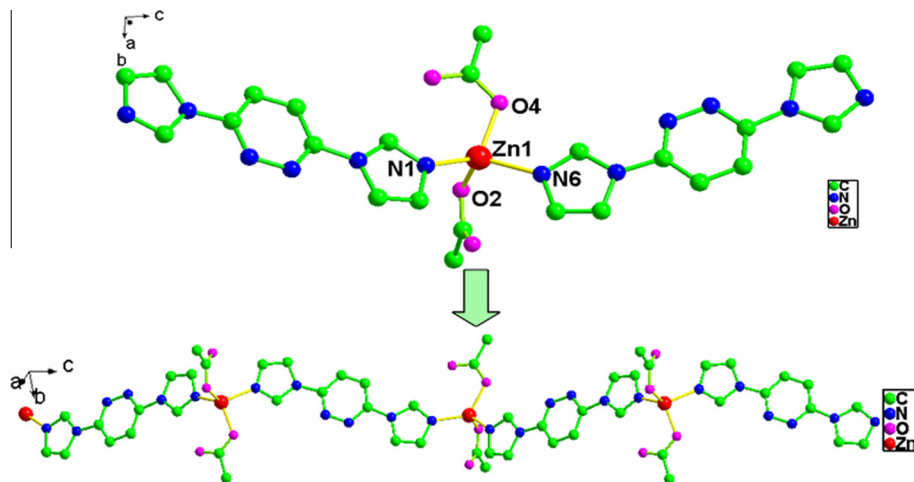


Fig. 2. View of the 1-D supramolecular chain of **2** (H atoms omitted for clarity).

3.2.3. $\{[ZnL(H_2O)_4](SO_4)\}_\infty$ (**3**) and $\{[CdL(H_2O)_4](SiF_6)\}_\infty$ (**6**)

Structural analyses are carried out that complexes **3** and **6** have similar 1-D structures. The coordination environment of Zn^{II} ion in **3** is also the same as that of Cd^{II} ion in **6**. Therefore, we just described detailedly the structure of complex **3**.

Complex **3** crystallizes in the monoclinic space group $P21/c$. Crystallographic data and experimental details for structural analyses were summarized in Table 1. In **3**, each Zn^{II} center is coordinated by two N atoms from two **L** ligands (Fig. 3) and four O atoms from water molecules. The N-Zn-N coordination angle is 101.72°, and it is smaller than that of **2**. The Zn-N bond distances are 2.134(7) Å and 2.160(7) Å (see Table 1 of Supplementary 1), respectively. The combination of Zn^{II} centers and rigid ligands form an infinite 1-D chain (Fig. 3). The two imidazole rings are coplanar with the central pyridazine ring. The **L** ligands, acting as bisconnector, link Zn^{II} to form the 1-D chain with the Zn···Zn distance of 12.961 Å. Resulting from such coordination mode, the $[ZnL(H_2O)_4]^{2+}$ unit has two positive charge. Obviously, the structural difference of **2** and **3** is attributable to the difference of counter anions, namely, CH_3COO^{2-} anions for **2** and SO_4^{2-} anions for **3**. The coordination ability of SO_4^{2-} anions are weaker than that of CH_3COO^{2-} anions, so the SO_4^{2-} anions did not show any bonding interactions with Zn^{II}, and only acted as counter anions for charge balance. In the same as **2**, all Zn^{II} centers are equivalent in **3**.

When the reaction of **L** with $CdSiF_6 \cdot 6H_2O$ was carried out in a H_2O/CH_3OH mixed solvent, complex **6** was obtained. Because the weaker coordination ability of SiF_6^{2-} anions, complex **6** formed the 1-D chain structure similar to **3**, (Fig. 3). The Cd^{II} center lies in a slightly distorted octahedral environment. Ligand **L** acts as a typical bridging ligand coordinating to the Cd^{II} ion with the Cd-N bond distances 2.295(2) and 2.312(2) Å, the N-Cd-N angel being 102.97(9)°, the neighboring non-bonding Cd···Cd distance connected by **L** is 13.303 Å. In the same as complex **3**, in **6**, SiF_6^{2-} anion does not show any bonding interactions with Cd^{II}, and only acts as a counter anion for charge balance.

3.2.4. $\{[CdL(AcO)_2](CH_3CH_2OH)\}_\infty$ (**5**)

To investigate the influence of counter anions in constructing coordination frameworks, **5** was obtained by the reaction of **L** with $Cd(AcO)_2 \cdot 2H_2O$. Complex **5** crystallizes in the orthorhombic space group $Pbca$. Selected bond lengths and angles were shown in Table 1 of Supplementary 1. X-ray single-crystal diffraction analyses revealed that **5** has an infinite grid structure consisting of the one Cd^{II} ion, two CH_3COO^{2-} anions, one free CH_3CH_2OH molecule and one **L** ligand. The Cd^{II} ion is six-coordinated to two N donors from two distinct **L** ligands [Cd(1)-N(6) = 2.2551(16) Å, Cd(1)-N

(1) = 2.2584(16) Å] and four O atoms of three distinct acetate anions. The structural difference of **4** and **5** is attributable to the difference of counter anions, namely, NO_3^- anions for **4** and CH_3COO^{2-} anions for **5**, and one acetate anion adopting bidentate chelating coordination mode and two adopting bidentate bridging coordination mode in **5** (Fig. 4a). Compared with complex **2**, **5** formed an infinite grid structure due to the bidentate bridging coordination mode of CH_3COO^{2-} anion.

The **L** ligand, acting as a bisconnector, links Cd^{II} to form the 1-D chain running along the *c*-axis with the Cd···Cd distance of 13.722 Å. At the same time, the 1-D chains were further assembled by the acetate anions via Cd-O bonds to form a infinite 2-D sheet (Fig. 4b).

3.2.5. $\{[Cu_2L_2(SO_4)_2(H_2O)_2](H_2O)\}_\infty$ (**7**)

Complex **7** crystallizes in the monoclinic space group $P21/c$, and selected bond distances and angles are listed in Table 1 of Supplementary 1. The asymmetric unit consists of two crystallographically independent Cu^{II} centers, two ligands **L**, two SO_4^{2-} anions, two coordinating water molecules and one free water molecule.

The Cu(1) center is linked to two distinct imidazole N donors of two **L** ligands in the cone roof, two O atoms from SO_4^{2-} anions [Zn(1)-O(1) = 2.121(3) Å] and one O atom from water molecule in the equatorial plane to complete its distorted trigonal bipyramidal geometries (Fig. 5a). The **L** ligand, acting as a bisconnector, links Cu(1) to form the 1-D chain with the Cu···Cu distance of 13.235 Å. At the same time, the 1-D chains were further assembled by the SO_4^{2-} anions via Cu-O bonds to form an infinite 2-D sheet (Fig. 5b).

The Cu(4) center is linked to two distinct imidazole N donors of two **L** ligands in the cone roof, two O atoms from SO_4^{2-} anions [Zn(1)-O(1) = 2.121(3) Å] and one O atom from water molecule in the equatorial plane to complete its distorted trigonal bipyramidal geometries (Fig. 5c). It is noticeable that the Cu(4) center is bridged by two oxygen atoms (O4) of SO_4^{2-} anions to form a binuclear unit and the O(4) of SO_4^{2-} anions adopts μ_2 bridging coordination modes (Fig. 5d). The binuclear unit was further assembled by the **L** via Cu-N bonds to form a 1-D chain (Fig. 5e). It should be pointed out that the 1-D chain and 2-D sheet form complicated structure of complex **7** (Fig. 5f).

3.3. Powder X-ray diffraction of the complexes

To confirm whether the crystal structures are truly representative of the bulk materials, X-ray powder diffraction (XRPD) experiments were carried out for complexes **1–7**. The XRPD

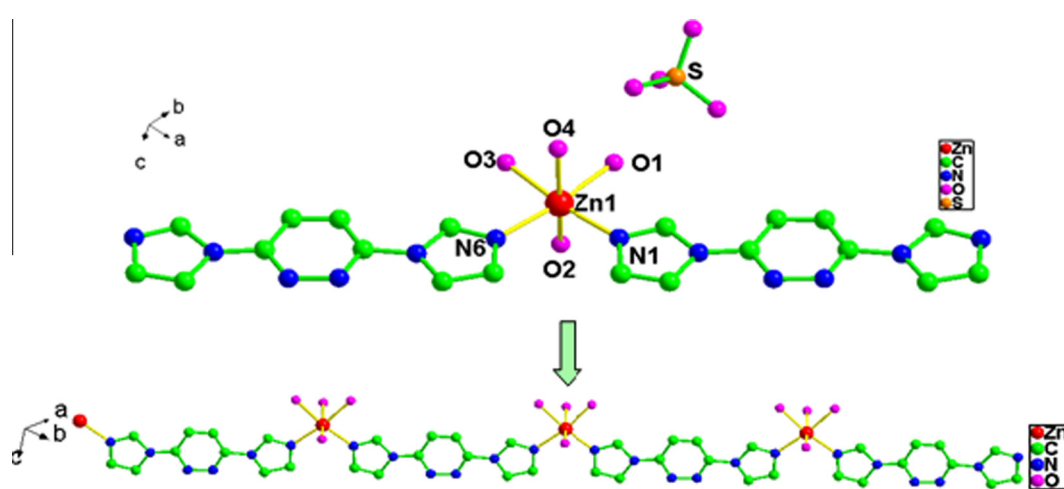


Fig. 3. View of 1-D supramolecular chain of **3** and **6** (H atoms omitted for clarity).

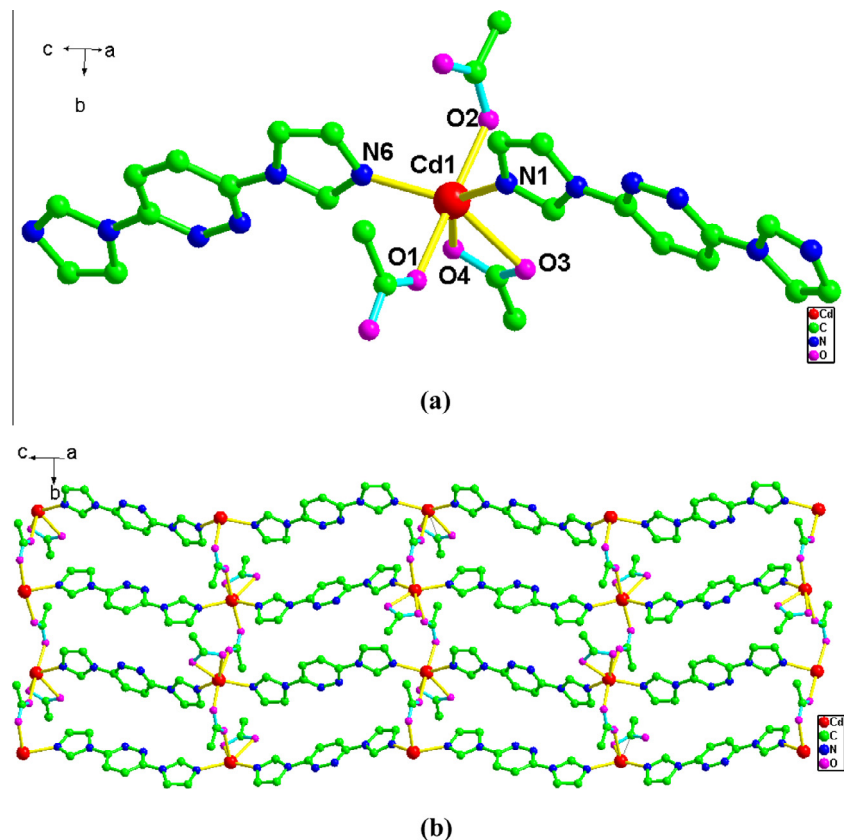


Fig. 4. View of (a) the coordination environment of Cd^{II} ions in **5** (b) the 2-D network structure of **5** (H atoms omitted for clarity).

experimental and computer-simulated patterns of the corresponding complexes are shown in Fig. S1 of Supplementary 2. Although the experimental patterns have a few unindexed diffraction lines and some are slightly broadened in comparison with those simulated from the single crystal modes, it still can be considered favorably that the bulk synthesized materials and the as-grown crystals were homogeneous for **1–7**.

3.4. Luminescent property

As is well known, the transition metal compounds exhibit changeable luminescence behaviors. The emission wavelength and luminescence mechanism can be significantly affected by organic ligands and their coordination modes [24]. The solid-state luminescence properties of complexes **1–6** as well as the free **L** ligand were investigated at room temperature under the same experimental conditions and their emission spectra are given in Supplementary 3. Upon excitation with 247 nm light, the free **L** ligand exhibits luminescence spectra with an emission maximum at 403 nm, which can be ascribed to ligand-centered electronic transition, that is, the $\pi^* \rightarrow n$ or $\pi^* \rightarrow \pi$ transition in nature according to the reported literature [25]. Complexes **1** and **6** all display strong fluorescent emission bands at 401 nm upon excitation at 250 nm, complexes **2** and **3** also show a single peak at 400 nm and 401 nm with $\lambda_{ex} = 247$ nm, respectively. Complexes **4** and **5** display strong fluorescent emission bands at 399 nm and 397 nm upon excitation at 246 nm, respectively. The above results reveal that the peaks of the emission spectra for **1–6** are very close to that of the free ligand, which can probably be attributed to the intraligand fluorescence originates from ligand-centered emission [26]. The significantly enhanced luminescence efficiency can be attributed to the ligand coordination to the metal centre, which enhances

the rigidity of the ligand and thus reduces the loss of energy through a radiationless pathway [24a,27].

3.5. Photocatalytic activity

It is well known that many complexes possess photocatalytic activities [28]. To evaluate the photocatalytic activities of complexes **1–6** were evaluated for the degradation of rhodamine B (RhB) (553 nm), methylene blue (MB) (664 nm), congo red (CR) (497 nm) and methyl orange (MO) (463 nm) in aqueous solutions. The photocatalytic reactions were performed as follows: 50 mg of the complexes was dispersed in 50 mL aqueous solution of RhB (10 mg L^{-1}) MB (10 mg L^{-1}) CR (10 mg L^{-1}) and MO (10 mg L^{-1}). Then the solution was exposed to UV irradiation from a 300 W high pressure mercury vapor lamp with circulating water cooling system at 10 cm distance between the liquid surface and the lamp. The samples of 5 mL were taken out every 30 min for UV measurement. By contrast, the control photocatalysis experiments of the three organic dyes aqueous solution were also performed under the same conditions without any catalyst.

These results suggest that **1–6** are inefficient catalysts for RhB, CR and MO degradation, and complex **6** can restrain the photodegradation of MB. However, complexes **1–5** are very efficient catalysts for MB degradation. When no catalyst was added, MB could be degraded by ca. 39% within 4 h under UV irradiation. The final results show that the degradation rate of MB is 80.0% for **1**, 77.6% for **2**, 92.1% for **3**, 77.5% for **4**, 82.2% for **5**, and the curves of absorbance of the MB solution degraded by **1–6** of under UV light see Fig. S1 of Supplementary 4, the absorption spectra of the MB solution during the decomposition reaction under UV irradiation with the presence of complexes **1–6** see Fig. S2 of Supplementary 4. The results indicate that **1–5** have photocatalytic

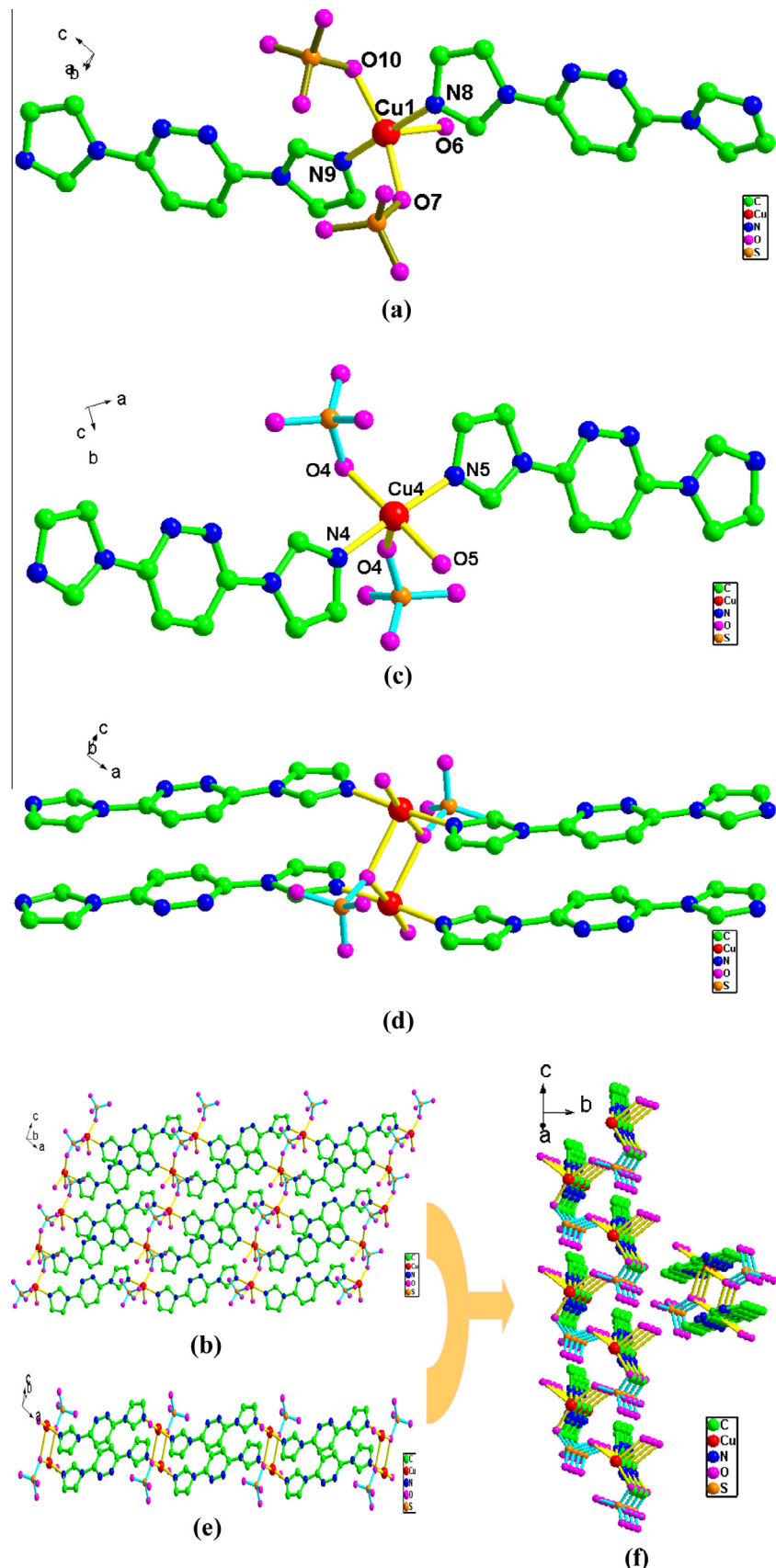


Fig. 5. View of (a) the coordination environment of Cu(1) center in **7** (b) the 2-D network structure of **7** (c) the coordination environment of Cu(2) center in **7** (d) the binuclear unit of **8** (e) the 1-D supramolecular chain in **7** (f) the whole structure of **7** (H atoms omitted for clarity).

activity and selectivity for the degradation of MB. The different photocatalytic performances of these complexes may be due to their different components and structures [29].

During the degradation process, the UV light irradiation may induce electron transfer from the highest occupied molecular orbital (HOMO) contributed by the oxygen and/or nitrogen 2p bonding orbital (valence band) to the lowest unoccupied molecular orbital (LUMO) contributed by an empty metal orbital (conduction band). Therefore, one electron was captured from water molecules to the HOMO in order to counteract this imbalance, and the water molecules were oxy-genated to generate the ·OH active radicals. As we all know, the ·OH active species could decompose MB effectively to complete the photocatalytic process [30].

4. Conclusion

A series of new transitional metal-organic complexes have been synthesized and structurally characterized. These compounds show fascinating 0-D to 2-D structures. The structural diversities of the compounds indicate that the rigid 3,6-bis(*N*-imidazolyl) pyridazine ligand is a good candidate for the construction of coordination polymers with fascinating motifs. Additionally, the influences of the locality and amount of coordination atoms in the same ligands and counter anions on the resultant structures of their metal complexes are briefly discussed. Moreover, the ligand **L** and corresponding complexes display strong bluefluorescent emission at room temperature. This approach may be useful for the construction of a variety of new transition metal complexes and luminescent coordination polymers with novel structures. The photocatalytic activity and selectivity of complexes **1–5** prove that they may be good and stable photocatalysts for degradation of organic dyes.

Acknowledgment

This work was financially supported by the National Nature Science Foundation of China (No. 21361026).

Appendix A. Supplementary data

CCDC 1411168–1411173 and 1411175 contains the supplementary crystallographic data for **1**·[Zn**L**₄(OH)₂]_n, **2**·{[Zn**L**(AcO)₂]·(CH₃CH₂OH)}_n, **3**·{[Zn**L**(H₂O)₄](SO₄)}_n, **4**·{Cd**L**₄(OH)₂}_n, **5**·{[Cd**L**(AcO)₂]·(CH₃CH₂OH)}_n, **6**·{[Cd**L**(H₂O)₄](SiF₆)}_n and **7**·{[Cu₂**L**₂(SO₄)₂(H₂O)₂]·(H₂O)}_n respectively. These data can be obtained free of charge via <http://www.ccdc.cam.ac.uk/conts/retrieving.html>, or from the Cambridge Crystallographic Data Centre, 12 Union Road, Cambridge CB2 1EZ, UK; fax: (+44) 1223 336 033; or e-mail: deposit@ccdc.cam.ac.uk. Supplementary data associated with this article can be found, in the online version, at <http://dx.doi.org/10.1016/j.poly.2016.03.025>.

References

- [1] (a) L.J. Barbour, G.W. Orr, J.L. Atwood, *Nature* 393 (1998) 671;
 (b) X. Li, X. Xu, D. Yuanb, X. Weng, *Chem. Commun.* 48 (2012) 9014;
 (c) M. Mascal, L. Infantes, J. Chisholm, *Angew. Chem., Int. Ed.* 45 (2006) 32;
 (d) X.D. Chen, X.H. Zhao, M. Chen, D. Miao, *Chem. Eur. J.* 15 (2009) 12974;
 (e) S. Das, P.K. Bharadwaj, *Inorg. Chem.* 45 (2006) 5257;
 (f) K. Maity, T. Kundu, R. Banerjeeb, K. Biradha, *CrystEngComm* 17 (2015) 4439;
 (g) J. Bai, H.L. Zhou, P.Q. Liao, W.X. Zhang, X.M. Chen, *CrystEngComm* 17 (2015) 4462.
- [2] (a) D. Tian, Q. Chen, Y. Li, Y.H. Zhang, Z. Chang, X.H. Bu, *Angew. Chem., Int. Ed.* 53 (2014) 837;
 (b) H. Wang, J. Xu, D.S. Zhang, Q. Chen, R.M. Wen, Z. Chang, X.H. Bu, *Angew. Chem., Int. Ed.* 54 (2015) 5966;
 (c) J.R. Li, J. Sculley, H.C. Zhou, *Chem. Rev.* 2 (2012) 869;
 (d) M. Yoon, R. Srirambalaji, K. Kim, *Chem. Rev.* 2 (2012) 1196.
- [3] (a) H.H. Li, Z. Niu, L. Chen, H.B. Jiang, Y.P. Wang, P. Cheng, *CrystEngComm* 5 (2014) 3468;
 (b) B. Li, H.M. Wen, W. Zhou, B. Chen, *J. Phys. Chem. Lett.* 5 (2014) 3468;
 (c) H. Furukawa, K.E. Cordova, M. O'Keeffe, O.M. Yaghi, *Science* 341 (2013) 1230444.
- [4] (a) G.P. Zhou, Y.L. Yang, R.Q. Fan, W. Cao, B. Yang, *CrystEngComm* 14 (2012) 193;
 (b) H.Y. Wu, Q.H. Gong, D.H. Olson, J. Li, *Chem. Rev.* 112 (2012) 836;
 (c) S. Kitagawa, R. Kitaura, S. Noro, *Angew. Chem., Int. Ed.* 43 (2004) 2334;
 (d) M.W. Zhang, M. Bosch, T. Gentle, H.C. Zhou, *CrystEngComm* 16 (2014) 4069;
 (e) C.B. Tian, H.B. Zhang, S.W. Du, *CrystEngComm* 16 (2014) 4059.
- [5] (a) X.Y. Wan, F.L. Jiang, L. Chen, J. Pan, K. Zhou, K.Z. Su, J.D. Pang, G.X. Lyu, M.C. Hong, *CrystEngComm* 17 (2015) 3829;
 (b) W. Zhang, R.G. Xiong, *Chem. Rev.* 2 (2012) 1163;
 (c) H.C. Zhou, J.R. Long, O.M. Yaghi, *Chem. Rev.* 2 (2012) 673.
- [6] (a) S. Hu, K.H. He, M.H. Zeng, H.H. Zou, Y.M. Jiang, *Inorg. Chem.* 47 (2008) 5218;
 (b) S.M. Chen, Y.F. Chen, R. Lin, X.P. Lei, J. Zhang, *CrystEngComm* 15 (2013) 10423;
 (c) X.L. Wang, C.H. Gong, J.W. Zhang, L.L. Hou, J. Luan, G.C. Liu, *CrystEngComm* 16 (2014) 7745;
 (d) D. Rankine, A. Avellaneda, M.R. Hill, C.J. Doonan, C.J. Sumby, *Chem. Commun.* 48 (2012) 10328.
- [7] (a) H.Y. An, L. Wang, Y. Hu, F. Fei, *CrystEngComm* 17 (2015) 1531;
 (b) W. Yuan, T. Frisčić, D. Apperley, S.L. James, *Angew. Chem., Int. Ed.* 49 (2010) 3916;
 (c) B. Zheng, J.F. Bai, Z.X. Zhang, *CrystEngComm* 12 (2010) 49.
- [8] Z.X. Zhao, Y.W. Li, S.J. Liu, L.F. Wang, Z. Chang, J. Xu, Y.H. Zhang, *CrystEngComm* 17 (2015) 4301.
- [9] K. Liu, B.H. Ma, X.L. Guo, D.X. Ma, L.K. Meng, G. Zeng, F. Yang, G.H. Li, Z. Shi, S.H. Feng, *CrystEngComm* 17 (2015) 5054.
- [10] (a) J.L. Zhuang, M. Kind, C.M. Grytz, F. Farr, M. Diefenbach, S. Tussupbayev, M. C. Holthausen, A. Terfort, *J. Am. Chem. Soc.* 137 (2015) 8237;
 (b) G.B. Li, J.R. He, M. Pan, H.Y. Deng, J.M. Liu, C.Y. Su, *Dalton Trans.* 41 (2012) 4626.
- [11] (a) W.T. Yang, H.Y. Wu, R.X. Wang, Q.J. Pan, Z.M. Sun, H.J. Zhang, *Inorg. Chem.* 51 (2012) 11458;
 (b) W.T. Yang, T. Tian, H.Y. Wu, Q.J. Pan, S. Dang, Z.M. Sun, *Inorg. Chem.* 52 (2013) 2736.
- [12] (a) F.G. Li, Y.G. Bi, W.Y. Zhao, T.L. Zhang, Z.N. Zhou, L. Yang, *Inorg. Chem.* 54 (2015) 2050;
 (b) H.M. He, Y. Song, F.X. Sun, N. Zhao, G.S. Zhu, *Cryst. Growth Des.* 15 (2015) 2033;
 (c) Y.X. Guo, X. Feng, T.Y. Han, S. Wang, Z.G. Lin, Y.P. Dong, B. Wang, *J. Am. Chem. Soc.* 136 (2014) 15485.
- [13] (a) M.L. Deng, P. Yang, X.F. Liu, B. Xia, Z.X. Chen, Y. Ling, L.H. Weng, Y.M. Zhou, J.Y. Sun, *Cryst. Growth Des.* 15 (2015) 1526;
 (b) H. Ibrahim, C. Gibard, C. Hesling, R. Guillot, L. Morel, A. Gautier, F. Cisnetti, *Dalton Trans.* 43 (2014) 6981.
- [14] (a) D.Z. Wang, T.L. Hu, J.P. Zhao, X.H. Bu, *CrystEngComm* 12 (2010) 3587;
 (b) D.Z. Wang, C.S. Liu, J.R. Li, L. Li, Y.F. Zeng, X.H. Bu, *CrystEngComm* 9 (2007) 289;
 (c) D.Z. Wang, *Polyhedron* 35 (2012) 142;
 (d) D.Z. Wang, Q. Zhang, J.B. Zhang, Y.G. Wu, L.H. Cao, P.Y. Ma, *Polyhedron* 42 (2012) 216.
- [15] (a) H. Li, G.C. Xu, L. Zhang, J.X. Guo, D.Z. Jia, *Polyhedron* 55 (2013) 209;
 (b) G.C. Xu, L. Zhang, Y.H. Zhang, J.X. Guo, M.Q. Shi, D.Z. Jia, *CrystEngComm* 15 (2013) 2873;
 (c) L. Zhang, G.C. Xu, Y. Yang, J.X. Guo, D.Z. Jia, *Dalton Trans.* 42 (2013) 4248.
- [16] C.H. Ke, G.R. Lin, B.C. Kuo, H.M. Lee, *Cryst. Growth Des.* 12 (2012) 3758.
- [17] (a) X.X. Wang, Y.J. Ma, H.H. Li, G.H. Cui, *Transition Met. Chem.* 40 (2015) 99;
 (b) H.F. Zhu, J. Fan, T. Okamura, W.Y. Sun, N. Ueyama, *Cryst. Growth Des.* 5 (2005) 289.
- [18] (a) J.S. Hu, Y.J. Shang, X.Q. Yao, L. Qin, Y.Z. Li, Z.J. Guo, H.G. Zheng, Z.L. Xue, *Cryst. Growth Des.* 10 (2010) 4135;
 (b) S.S. Chen, Z.H. Chen, J. Fan, T. Okamura, Z.S. Bai, M.F. Lv, W.Y. Sun, *Cryst. Growth Des.* 12 (2012) 2315.
- [19] (a) F.Y. Yi, W. Yang, Z.M. Sun, *J. Mater. Chem.* 22 (2012) 23201;
 (b) F. Guo, B.Y. Zhu, M.L. Liu, X.L. Zhang, J. Zhang, J.P. Zhao, *CrystEngComm* 15 (2013) 6191;
 (c) L. Chen, L. Zhang, S.L. Li, Y.Q. Qiu, K.Z. Shao, X.L. Wang, Z.M. Su, *CrystEngComm* 15 (2013) 8214;
 (d) Q.X. Yang, X.Q. Chen, J.H. Cui, J.S. Hu, M.D. Zhang, L. Qin, G.F. Wang, Q.Y. Lu, H.G. Zheng, *Cryst. Growth Des.* 12 (2012) 4072.
- [20] (a) L.M. Fan, X.T. Zhang, Z. Sun, W. Zhang, Y.S. Ding, W.L. Fan, L.M. Sun, X. Zhao, H. Lei, *Cryst. Growth Des.* 13 (2013) 2462;
 (b) F.L. Hu, W. Wu, P. Liang, Y.Q. Gu, L.G. Zhu, H. Wei, J.P. Lang, *Cryst. Growth Des.* 13 (2013) 5050;
 (c) Z.X. Li, T.L. Hu, H. Ma, Y.F. Zeng, C.J. Li, M.L. Tong, X.H. Bu, *Cryst. Growth Des.* 10 (2010) 1138.
- [21] A.X.S. Bruker, SAINT Software Reference Manual, 1998. Madison, WI.
- [22] G.M. Sheldrick, SHELXL NT Version 5.1. Program for Solution and Refinement of Crystal Structures, University of Göttingen, Germany, 1997.
- [23] G.M. Sheldrick, SADABS Siemens Area Detector Absorption Correction Program, University of Gottingen, Gottingen, Germany, 1994.

- [24] (a) L.X. Cai, C. Chen, B. Tan, Y.J. Zhang, X.D. Yang, J. Zhang, *CrystEngComm* 17 (2015) 2353;
(b) D.L. Phillips, C.M. Che, K.H. Leung, Z. Mao, M.C. Tse, *Chem. Rev.* 249 (2005) 1476;
(c) Y.J. Mu, G. Han, S.Y. Ji, H.W. Hou, Y.T. Fan, *CrystEngComm* 13 (2011) 5943.
- [25] (a) Y.J. Cui, Y.F. Yue, G.D. Qian, B.L. Chen, *Chem. Rev.* 112 (2012) 1126;
(b) Z.P. Deng, L.H. Huo, H.L. Qi, L.N. Zhu, H. Zhao, S. Gao, *CrystEngComm* 13 (2011) 4218;
(c) T.L. Hu, Y. Tao, Z. Chang, X.H. Bu, *Inorg. Chem.* 50 (2011) 10994.
- [26] (a) R.H. Wang, D.Q. Yuan, F.L. Jiang, L. Han, Y.Q. Gong, M.C. Hong, *Cryst. Growth Des.* 6 (2006) 1351;
(b) H. Wu, W. Dong, H.Y. Liu, J.F. Ma, S.L. Li, J. Yang, Y.Y. Liu, Z.M. Su, *Dalton Trans.* 39 (2008) 5331.
- [27] (a) Z.R. Pan, H.G. Zheng, T.W. Wang, Y. Song, Y.Z. Li, Z.J. Guo, S.R. Batten, *Inorg. Chem.* 47 (2008) 9528;
(b) H.Y. Wang, S. Gao, L.H. Huo, S.W. Ng, J.G. Zhao, *Cryst. Growth Des.* 8 (2008) 665.
- [28] (a) L. Liu, J. Ding, C. Huang, M. Li, H.W. Hou, Y.T. Fan, *Cryst. Growth Des.* 14 (2014) 3035;
(b) J.S. Qin, S.R. Zhang, D.Y. Du, P. Shen, S.J. Bao, Y.Q. Lan, Z.M. Su, *Chem. Eur. J.* 20 (2014) 5625;
(c) X.L. Wang, N.L. Chen, G.C. Liu, A.X. Tian, X.T. Sha, K.F. Ma, *Inorg. Chim. Acta* 432 (2015) 128;
(d) M. Dai, H.X. Li, J.P. Lang, *CrystEngComm* 17 (2015) 4741.
- [29] (a) X. Zhou, P. Liu, W.H. Huang, M. Kang, Y.Y. Wang, Q.Z. Shi, *CrystEngComm* 15 (2013) 8125;
(b) W.Q. Kan, B. Liu, J. Yang, Y.Y. Liu, J.F. Ma, *Cryst. Growth Des.* 12 (2012) 2288.
- [30] (a) X.L. Wang, X.T. Sha, G.C. Liu, N.L. Chen, Y. Tian, *CrystEngComm* 17 (2015) 7290;
(b) J.Y. Zhang, Y.Y. Xing, Q.W. Wang, N. Zhang, W. Deng, E.Q. Gao, *J. Solid State Chem.* 232 (2015) 19.